

Structural analysis of three His32 mutants of DsbA: Support for an electrostatic role of His32 in DsbA stability

LUKE W. GUDDAT,¹ JAMES C. A. BARDWELL,² RUDI GLOCKSHUBER,³
MARTINA HUBER-WUNDERLICH,³ THOMAS ZANDER,² AND JENNIFER L. MARTIN¹

¹Centre for Drug Design and Development, University of Queensland, Brisbane, QLD 4072, Australia

²Department of Biology, University of Michigan, Ann Arbor, Michigan 48109-1048

³Institut für Molekularbiologie und Biophysik, ETH-Hönggerberg, CH-8093 Zürich, Switzerland

(RECEIVED February 14, 1997; ACCEPTED May 20, 1997)

Abstract

DsbA, a 21-kDa protein from *Escherichia coli*, is a potent oxidizing disulfide catalyst required for disulfide bond formation in secreted proteins. The active site of DsbA is similar to that of mammalian protein disulfide isomerases, and includes a reversible disulfide bond formed from cysteines separated by two residues (Cys30–Pro31–His32–Cys33). Unlike most protein disulfides, the active-site disulfide of DsbA is highly reactive and the oxidized form of DsbA is much less stable than the reduced form at physiological pH.

His32, one of the two residues between the active-site cysteines, is critical to the oxidizing power of DsbA and to the relative instability of the protein in the oxidized form. Mutation of this single residue to tyrosine, serine, or leucine results in a significant increase in stability (of ~5–7 kcal/mol) of the oxidized His32 variants relative to the oxidized wild-type protein.

Despite the dramatic changes in stability, the structures of all three oxidized DsbA His32 variants are very similar to the wild-type oxidized structure, including conservation of solvent atoms near the active-site residue, Cys30. These results show that the His32 residue does not exert a conformational effect on the structure of DsbA. The destabilizing effect of His32 on oxidized DsbA is therefore most likely electrostatic in nature.

Keywords: DsbA; mutagenesis; oxidoreductase; protein crystallography; protein stability; thioredoxin fold

The efficient introduction of disulfide bonds into newly translocated proteins in the periplasm of *Escherichia coli* is catalyzed by the redox protein DsbA (Bardwell et al., 1991, 1993; Akiyama et al., 1992). In eukaryotes, the protein that catalyzes the equivalent reaction in the endoplasmic reticulum is protein disulfide isomerase (PDI) (Freedman, 1989). Despite differences in size and complexity, DsbA (21 kDa) and PDI (2×57 kDa) both incorporate the thioredoxin fold in their structure. The PDI sequence has two thioredoxin oxidoreductase domains per monomer (Edman et al., 1985; Kemmink et al., 1996) and DsbA incorporates a single thioredoxin domain (with an additional helical domain inserted into the thioredoxin domain). The sequence identity between DsbA and thioredoxin is only about 10% (Martin et al., 1993a). The redox active site of the thioredoxin domain in both proteins includes the characteristic Cys–X–X–Cys motif, in which the two cysteines can reversibly form a disulfide bond.

DsbA and PDI are both strong oxidants, which is reflected in their low redox equilibrium constants with glutathione (K_{ox}) of ~0.1 mM (Wunderlich & Glockshuber, 1993b; Zapun et al., 1993) and ~1 mM (Lundström & Holmgren, 1993; Darby & Creighton, 1995), respectively. In contrast, the K_{ox} of the general protein reductant thioredoxin is 10 M (Lin & Kim, 1989). The highly oxidizing nature of DsbA is critical for its disulfide catalysis function and has been postulated to be a result of the very low pK_a of Cys30, the more N-terminal of the two redox active-site cysteines (Nelson & Creighton, 1994; Grauschof et al., 1995). The usual pK_a value for a cysteine is ~9, but that of DsbA Cys30 is 3.5 (Nelson & Creighton, 1994). The extremely low pK_a of DsbA makes it highly oxidizing by facilitating the exit from disulfide exchange reactions with Cys30 in the reduced thiolate ion form. Furthermore, the reduced form of the protein has been shown to be *more stable* than the disulfide-bonded form of DsbA (Wunderlich et al., 1993; Zapun et al., 1993), in contrast to most protein disulfides that enhance protein stability.

The unusual properties of the DsbA active-site disulfide arise, at least in part, from the two amino acids between the cysteines of the active site. These two residues are characteristically different

Reprint requests to: Jennifer L. Martin, Centre for Drug Design and Development, University of Queensland, Brisbane, QLD 4072, Australia; e-mail: J.Martin@mailbox.uq.oz.au.

between thioredoxin-like redox protein families, yet are highly conserved within each family (thioredoxin Cys–Gly–Pro–Cys; glutaredoxin Cys–Pro–Tyr–Cys; DsbA Cys–Pro–His–Cys; PDI Cys–Gly–His–Cys). For example, by mutating the proline residue in thioredoxin to histidine (as in PDI) the redox potential is increased by 35 mV (Krause et al., 1991) to become more like that of PDI. Mutations between the cysteines in DsbA can result in redox equilibrium constants that differ by three orders of magnitude from that measured for wild-type (*wt*) DsbA (Grausopf et al., 1995).

Of prime importance in DsbA function and stability is the histidine residue, His32, between the two active-site cysteines. The properties of three His32 mutants—tyrosine, serine, and leucine—are given in Table 1. All three mutants are less oxidizing than *wt* DsbA as shown by the altered K_{eq} values (which are increased 10–50 fold). In addition, there are large stability changes in the oxidized and reduced forms of the mutant enzymes compared with *wt* DsbA. For example, the single amino acid change that gives rise to H32Y, the glutaredoxin variant of DsbA, results in a reversal of the *wt* stability. Thus, in contrast to *wt* DsbA, the oxidized form of H32Y DsbA is the more stable of the two redox forms. Furthermore, the oxidized form of H32Y is significantly more stable (by 6.8 kcal/mol) than the oxidized form of the *wt* enzyme.

The other two His32 mutants were identified from an *in vivo* screen for DsbA mutants with altered redox activity (Grausopf et al., 1995). Conversion of His32 to leucine (H32L DsbA) or serine (H32S DsbA) results in a protein with a significantly more stable oxidized form and a more stabilized reduced form. Although both oxidized and reduced forms are stabilized relative to the equivalent forms in *wt* DsbA, the oxidized form of both mutants is stabilized substantially more. This results in a smaller difference in stability between the oxidized and reduced forms ($\Delta\Delta G$) of the mutants compared with *wt*. This smaller $\Delta\Delta G$ can be used to predict that these mutants should have a less oxidizing redox equilibrium constant than has *wt* DsbA. The measured redox equilibrium constants of these mutants follow this prediction.

The data from the present work show that, compared with other residue types, a histidine at position 32 in the sequence destabilizes the oxidized form of DsbA by ~5–7 kcal/mol. This destabilization of oxidized DsbA by His32 could be a conformational effect, a change in solvent structure around the active-site, or an electrostatic effect. Based on our analysis of the crystal structures of the oxidized forms of three DsbA His32 mutants, it appears that an electrostatic effect is the most likely mechanism for destabilization of oxidized DsbA by histidine at position 32.

Results

Structures of the oxidized His32 mutants of DsbA

The crystal structures of the three His32 DsbA mutants in the oxidized form have been determined to high resolution (Table 2). These structures are isomorphous with the oxidized *wt* DsbA crystal structure allowing a direct comparison to be made between these structures.

For the comparison of the His32 mutant structures with *wt* DsbA, we used the structure of oxidized *wt* DsbA refined to 1.7 Å (Guddat et al. 1997; PDB accession code 1FVK). This structure is similar to that refined to 2.0 Å (Martin et al., 1993a; PDB accession code 1DSB).

Structural comparison with *wt* oxidized DsbA shows that mutation of the critical His32 residue does not alter the structure. The structures of all three His32 mutants are essentially identical to *wt* oxidized DsbA, with r.m.s. deviations in $C\alpha$ positions compared with *wt* DsbA of 0.10 Å for H32Y DsbA, 0.21 Å for H32L DsbA, and 0.17 Å for H32S DsbA.

Analysis of the active-site disulfide

The active-site disulfide of DsbA is located at the N-terminal end of the first helix in the thioredoxin domain and comprises residues Cys30–Pro31–His32–Cys33. In this crystal form, the active-site cysteines are oxidized to form a disulfide, and the two monomers in the asymmetric unit are oriented such that the active sites face each other. As in all known structures of the thioredoxin family of disulfide oxidoreductases, the Cys30–Cys33 disulfide bridges in *wt* DsbA are right-handed for both monomers of the asymmetric unit. In *wt* DsbA, the χ_{ss} values are 80° and 76° and the $C\alpha$ – $C\alpha$ distances are 5.1 Å and 5.2 Å, respectively.

The disulfide conformation of DsbA is one of the least populated in a study of disulfide bond conformation (three out of 43; Srinivasan et al., 1990) yet is highly conserved within the thioredoxin redox protein family. This could be a result of geometric restrictions imposed by disulfide bond formation between cysteines separated by only two residues (the number of intervening residues in the disulfides studied by Srinivasan et al. varies from four to 129).

In all three His32 mutant DsbA structures, the disulfide bridge maintains the right-handed conformation of *wt* oxidized DsbA. The active-site atoms of residues 30–33 are identically placed to those in the *wt* structure, with r.m.s. deviations for all pairs of

Table 1. Properties of His32 mutants

	<i>wt</i> DsbA ^a	H32Y DsbA ^b	H32L DsbA ^a	H32S DsbA ^a
K_{eq} (mM) ^c	0.12 ± 0.004	1.8 ± 0.026	1.6 ± 0.004	6.1 ± 0.05
ΔG_{ox} (kcal/mol) ^d	-7.0 ± 0.7	-13.8 ± 1.05	-12.3 ± 1.1	-12.2 ± 0.6
ΔG_{red} (kcal/mol) ^d	-11.1 ± 0.3	-11.6 ± 0.48	-15.7 ± 1.7	-14.7 ± 0.3
p <i>K_a</i> of Cys 30 ^e	3.42 ± 0.18	3.75 ± 0.06	4.42 ± 0.10	4.87 ± 0.05^f

^aData from Grausopf et al. (1995) and this work.

^b K_{eq} and p*K_a* data from Wunderlich (1994), stability data from M. Huber-Wunderlich and R. Glockshuber (manuscript in preparation). Methods are described in the text.

^cRedox equilibrium constant with glutathione, measured at pH 7 and 30 °C as described in Wunderlich and Glockshuber (1993b).

^dFree energy of folding of oxidized and reduced DsbA, measured as described in Wunderlich et al. (1993).

^ep*K_a* of the thiol of Cys-30, determined as described in Nelson and Creighton (1994).

^fP. Korber and J. C. A. Bardwell (unpublished work).

Table 2. Crystallographic statistics

Data measurement	H32Y DsbA	H32L DsbA	H32S DsbA
Resolution limits (Å)	50.0–2.06	50.0–2.00	50.0–1.90
No. of observations ($I > 1\sigma I$)	74,395	84,044	97,285
No. of reflections ($I > 1\sigma I$)	26,611	28,490	33,192
R_{sym} (outer shell)	0.056 (0.219)	0.081 (0.298)	0.054 (0.323)
$I/\sigma I$ (outer shell)	17.3 (3.84)	13.6 (2.36)	17.6 (2.6)
Completeness (outer shell)	91.1% (84.1%)	91.5% (83.0%)	94.1% (84.1%)
<i>Refinement</i>			
No. of reflections ($F > 1\sigma(F)$)	26,334	27,226	33,192
R -factor ($F > 1\sigma(F)$)	0.180	0.176	0.182
R -free ($F > 1\sigma(F)$)	0.218	0.220	0.216
<i>Rms deviations from ideal</i>			
Bond length (Å)	0.007	0.007	0.007
Bond angle (°)	1.38	1.14	1.13
Dihedral angle (°)	21.98	22.8	22.7
Improper angle (°)	1.03	1.13	1.08
Average B-factor (Å ²)	35.9	33.5	33.8
No. of water molecules	164	157	167

$R_{\text{sym}} = \sum|I - \langle I \rangle|/\sum\langle I \rangle$. Outer shell for H32Y is 2.06 to 2.25 Å; H32L, 2.00 to 2.07 Å; and H32S, 1.90 to 1.97 Å. R -factor = $\sum|F_{\text{obs}} - F_{\text{calc}}|/\sum F_{\text{obs}}$. R -free as defined by Brünger (1992a), using 10% of the data.

structures ($\text{C}\alpha$, $\text{C}\beta$, C, O, N, and Sγ atoms) varying between 0.04 and 0.09 Å.

This structural equivalence between mutants with very different redox properties provides strong support for an electrostatic rather than a structural role of His32 in determining the redox properties of DsbA (see Discussion).

Conformational analysis of residue 32

As there was no significant change in DsbA structure in the His32 mutants, we examined in detail the conformation of the mutated residue 32. The conformational preference of amino acid side chains in proteins has been analyzed using high resolution protein crystal structures (McGregor et al., 1987; Ponder & Richards, 1987). Generally, three rotamers are found for the χ_1 angle of all amino acid side chains (defining the rotation about the $\text{C}\alpha$ – $\text{C}\beta$ bond), these being gauche– (g^- , $\sim 60^\circ$), trans (t , $\sim 180^\circ$) and gauche+ (g^+ , $\sim -60^\circ$). The preference for each rotamer varies depending on residue type and secondary structure. Analysis of the rotamer distribution for residues at the N-termini of helices (McGregor et al., 1987) is particularly useful for the investigation of residue 32 in DsbA, the mutated amino acid, since it is situated near the N-terminus of the α -helix (position N2 in the nomenclature of Richardson & Richardson, 1988). In this context, a g^+ conformation of residue 32 places the side chain into solvent, a t rotamer positions it near hydrophobic residues from the core of the protein, and a g^- rotamer places it over the disulfide bond (Fig. 1). Furthermore, rotation of residue 32 in monomer A is unrestricted around χ_1 (all three rotamers are possible). However, rotation of residue 32 of monomer B is restricted (the g^+ rotamer is disallowed) due to steric constraints imposed by atoms from the non-crystallographic symmetry related monomer A (Fig. 1).

Histidine residues near the N-termini of helices prefer to adopt the g^+ rotamer (54%), although the t and g^- rotamers are found

in lower, but equal, proportion (23%) (McGregor et al., 1987). His32 in the *wt* DsbA structure is observed in two conformations (Fig. 2a; Table 3): The unrestricted His A32 adopts the most favored g^+ conformation and His B32 has the t conformation. The His A32 side chain points towards solvent, is poorly ordered, and makes interactions only with waters (Table 3). Conversely, His B32 points into the protein, is shielded from bulk solvent by monomer A, is well-ordered, and is stabilized by hydrogen bonds to a symmetry-related protein atom and a water, and by interactions

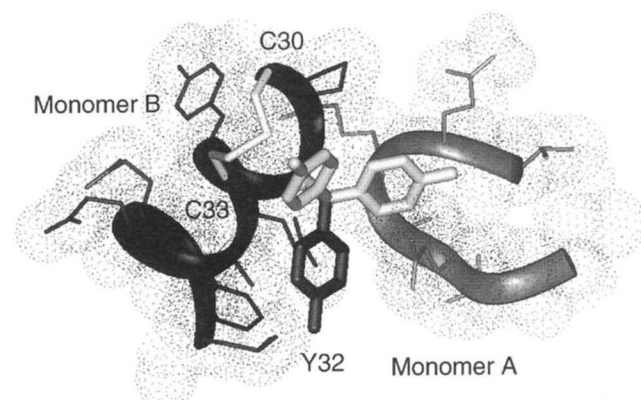


Fig. 1. The three χ_1 side-chain rotamers of residue 32 in DsbA. The region around DsbA monomer B active site is shown. The three side-chain rotamers of residue 32 are g^+ (light gray, pointing to the right), t (black, pointing down), and g^- (dark gray, pointing to the left). The g^+ conformation is accessible in monomer A but disallowed in monomer B because of steric constraints imposed by monomer A (dark gray). Residues shown from the active-site helix of monomer B are Cys30, Pro31, Tyr32, Cys33, Tyr34, Gln35, Phe36, Glu37, Glu38, and Leu40 (Cys30, Tyr32, and Cys33 are labeled). Residues shown from monomer A are Val96 (top right), Gln97, Lys98, Thr99, Gln100, and Thr101.

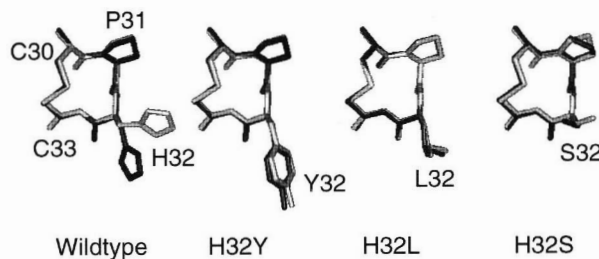


Fig. 2. Conformation of residue 32. The active-site residues are shown for monomer A (light) and monomer B (dark) for *wt* and His32 mutant DsbA structures.

with Phe B36 and Pro B151. These results show that His32 in *wt* DsbA preferentially adopts the *g+* conformation (as observed in other protein structures) but can adopt the *t* conformation where steric restrictions preclude *g+*.

Similar to the observation for histidines, a tyrosine residue at the N-terminal end of a helix is most likely to be found as the *g+* rotamer (62%). However, of the remaining two rotamers, *t* (31%) is clearly preferred over *g-* (8%) (McGregor et al., 1987). The structure of H32Y DsbA shows that the mutated residue Tyr32 is in the *t* conformation in both monomers (Fig. 2b; Table 3). Thus, in the A monomer, where rotation of residue 32 is not enforced by crystal contacts, Tyr 32 adopts a different rotamer conformation to His 32.

The *t* conformation in this instance is probably adopted to minimize solvent accessibility of the tyrosine side chain. In both A and B monomers, the side chain of Tyr32 forms no hydrogen bonds but the aromatic ring is stabilized by non-covalent interactions with Phe36 and Pro151. The side-chain accessible surface area of Tyr A32 and B32 is 83 and 16 Å², respectively (Table 3). When Tyr A32 is rotated into the *g+* conformation, the side-chain accessible surface area is calculated to be 150 Å². Of the other 16 tyrosine residues in the DsbA crystal structure, the side-chain accessible surface area varies between 0 and 71 Å². Even in the more buried *t* conformation, Tyr A32 has a high average side-chain B-factor (50 Å²) compared with Tyr B32 (29 Å²) and compared with other tyrosine side-chains in the DsbA structure (21 - 44 Å²). Indeed, for all four DsbA structures, the side chain of residue 32 from monomer A has higher average B-factors and solvent accessibility than residue 32 from monomer B (which is shielded by monomer A).

The conformational preference of leucine residues at the N-termini of α -helices is roughly distributed between *t* (49%) and *g+* (46%), with a much lower preference for *g-* (5%) (McGregor et al., 1987). For H32L DsbA, residue 32 is found in the *t* conformation in both monomers (Fig. 2c). As with H32Y, the preference for this rotamer is probably a result of hydrophobic stabilization.

Finally, serine residues are unusual in their preference for the *g-* conformation (65%) over the *t* and *g+* conformations (18% each) at the N-termini of α -helices (McGregor et al., 1987). For H32S DsbA, the unrestricted A conformation adopts the *g+* conformation (Fig. 2d; Table 3), like that of His32 in *wt* DsbA. In this conformation, the hydroxyl of the Ser A32 side chain interacts with a solvent molecule. The B conformation of Ser32 adopts the preferred *g-* conformation and interacts with a solvent molecule, and possibly also with Cys30 Sy (3.8 Å). The *t* conformation for the serine side chain at residue 32 in DsbA is probably least preferred because of the hydrophobic environment.

Solvent structure around the active site

Mutation of His32 could theoretically cause changes to the stability and redox properties of DsbA by altering the solvent structure around the active site. However, the solvent structure is remarkably well-conserved throughout these four structures. In the *wt* DsbA structure, there are two water molecules (Wat1 and Wat2; Fig. 3) located near the Sy atom of the accessible active-site residue Cys30. Wat1 is present in *wt* and all three His32 mutant DsbA structures, in both A and B monomers. It forms a hydrogen bond with the main-chain N of residue 32 (2.8–3.0 Å), can interact with polar side chains of this residue (*wt* His32 and H32S), and also forms a hydrogen bond with Wat2 (2.7–3.0 Å). Wat1 is 3.7–3.9 Å distant from the Sy atom of Cys30, and its B-factor varies from 25–33 Å².

Wat2 is found in monomer B of all four structures, and in monomer A of H32S and H32L DsbA. It is positioned very near Sy of Cys30 (3.1–3.4 Å). In two of the DsbA molecules (*wt* monomer B and H32S monomer A), Wat2 also forms hydrogen bonds with a third water (Wat3) and with the main-chain O of Val150 (Fig. 3). In all cases, the B-factor of Wat2 (34–48 Å²) is somewhat higher than for Wat1 indicating that it is not as well-ordered.

The remarkable similarity of the solvent structure around the active site in all four DsbA structures suggests that alteration in the solvent structure is not responsible for changes in the redox properties of DsbA.

Phe36

As described above, there are no major structural changes in going from *wt* DsbA to any of the His32 DsbA mutants. There are changes in some surface-exposed side chains. However, these changes are not correlated with any other structural or functional changes and probably represent the range of motion available to these solvent accessible side chains. The only example of a concerted structural change for a buried residue appears to be Phe36. This residue has been implicated in substrate binding since it forms part of the proposed peptide-binding groove of DsbA (Martin et al., 1993a). Also, as described above, Phe36 can interact with residue 32 when the latter adopts the *t* conformation.

The movement in Phe 36 upon His32 mutation is relatively small, involving a χ_1 rotation of up to 20° (Fig. 4). The conformation of Phe36 is *g+* in all these DsbA structures, although the observed values of χ_1 (-89° to -108°) are somewhat removed from the preferred value (-60°). The small conformational changes in Phe36 are not a result of disorder, since the average side-chain B-factors are good (22–34 Å²). Rather, the observed changes appear to be a response to the changes occurring at the mutation site. Thus, compared with Phe36 of *wt* His32 DsbA (χ_1 -99°), Phe36 of H32Y moves further away from the active site (χ_1 -105° to -108°) to allow more room for the bulky Tyr32 side chain. Conversely, for the smaller side chains (Ser32, Leu32), Phe36 moves closer to the active site (χ_1 -89° to -94°) compared with that in *wt* DsbA. While these changes show that this buried residue can adapt to different environments in its vicinity (presumably an important requirement for a residue in a peptide binding site), they do not sufficiently explain the large changes in stability observed for the oxidized form of DsbA.

Strained domain connection

There are two domains in the three-dimensional structure of DsbA—a thioredoxin domain and a helical domain that is inserted

Table 3. Analysis of residue 32^a

	wt DsbA	H32Y DsbA	H32L DsbA	H32S DsbA
χ^1 ^b				
A	g+ (-75°)	t (-162°)	t (-166°)	g+ (-57°)
B	t (-162°)	t (-167°)	t (-172°)	g- (63°)
$\langle B \rangle$ ^c (Å ²)				
A	46	50	29	32
B	21	29	18	23
Solv. acc. ^d (Å ²)				
A	118	83	83	49
B	17	16	20	10
Side-chain interactions ^e				
A	Nδ1:Wat616 2.7 Å Nε2:Wat805 3.1 Å Phe36, Pro151	Phe36, Pro151	Phe36, Pro151	Oy:Wat616 2.9 Å Oy:Wat688 2.7 Å
B	Nδ1:Lys98 O 2.7 Å Phe36, Pro151	Phe36, Pro151	Phe36, Pro151	Oy:Wat688 2.7 Å

^aIn all cases, values for the two monomers, A and B, are listed separately.^b χ^1 : The conformation around the CαCβ bond of residue 32, categorized into gauche- (g-), trans (t), and gauche+ (g+) conformations. The specific angle is given in parentheses.^c $\langle B \rangle$: Average B-factor for side-chain atoms of residue 32.^dSolv. acc.: Solvent accessible surface area for side-chain atoms of residue 32, calculated using a probe radius of 1.4 Å.^eSide-chain interactions: Hydrogen bond interactions for side-chain atoms of residue 32 (Nδ1 and Nε2 for wt and Oy for H32S DsbA), using a cutoff of 3.2 Å. Residues that could form hydrophobic interactions are also listed. For wt and H32S structures, Wat616 and Wat688 are equivalent to Wat1, described in the text and shown in Fig 3.

into the thioredoxin domain (Martin et al., 1993a). One of the two connections between the thioredoxin and helical domains of DsbA is a type IV β-turn consisting of residues Phe63-Met64-Gly65-Gly66. The first residue of this turn, Phe63, has a strained main-chain conformation (N-Cα-C ~ 120°) in the *wt* DsbA structure and has been postulated to be a hinge point for domain motion (Guddat et al. 1997).

It was of interest to see whether the stability changes in the His32 mutants might be a result of the relief of strain in this "hinge" residue. However, all three His32 mutant structures retain the strained Phe63 main-chain conformation (120–123°). Thus, the stability differences between the oxidized form of *wt* DsbA and

His32 mutants is not due to a relaxation of this main-chain angle. It is likely that our understanding of the functional importance, or otherwise, of the strained main chain of Phe63 will depend upon the structure determination of the reduced form of DsbA.

Discussion

Although the thermodynamic stabilities of the three oxidized His32 DsbA variants are increased markedly compared to the oxidized *wt*, the analysis of the high-resolution crystal structures reveals no large changes in structure compared with the *wt* protein. The structural changes observed appear to be restricted to local rearrangements in the vicinity of the exchanged residue. Similar results have been observed previously for other proteins (Clarke et al., 1995; Jackson et al., 1995; Matthews, 1995). However, the oxidized DsbA variants H32Y, H32L, and H32S appear to be some of the most extreme examples known so far. The exchange of a single, surface-exposed residue stabilizes the oxidized protein by 5–7 kcal/mol compared with oxidized *wt* DsbA. The only structural consequence of the mutation to tyrosine, leucine, or serine is a difference in population of three possible conformations of the mutated side chain and a small displacement of a nearby phenylalanine residue. Thus, significant shifts in the stability of a protein upon mutation of a residue may not be accompanied by large conformational differences.

The detailed conformational analysis of residue 32 (based on data from Table 3) shows that the hydrophobic residues tyrosine and leucine at this position prefer to adopt a conformation that minimizes solvent accessibility. The analysis also reveals that the polar histidine and serine side chains have distinct conformational differences between monomers A and B in this crystal form. Since the active site of monomer B is constrained by the presence of a

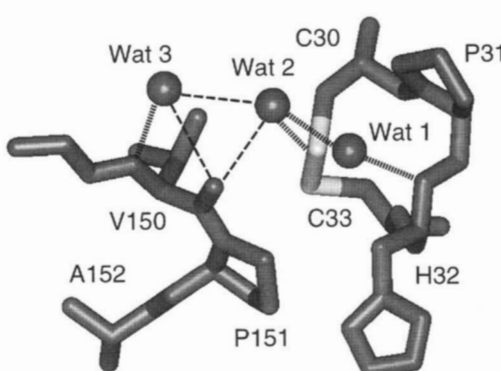


Fig. 3. Solvent structure near the active site of DsbA. Wat1, Wat2 and Wat3 are shown as spheres. Hydrogen bonds observed in all four structures are shown as thick dashed lines (=====). Hydrogen bonds that are not observed in all structures are shown as thin dashed lines (----).

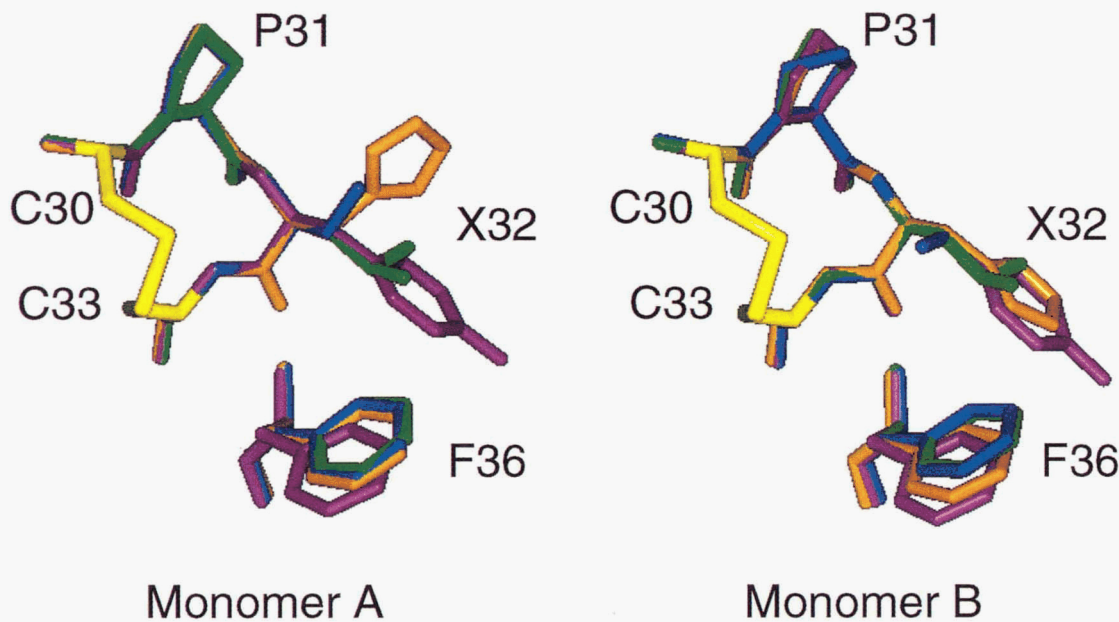


Fig. 4. Position of Phe36 in His32 mutants of DsbA. The region around the active site of monomer A and B is shown superimposed for *wt* DsbA (orange), H32Y DsbA (purple), H32L DsbA (green), H32S DsbA (blue). The active-site disulfide of all the DsbA structures is shown in yellow, and residues 30–33 are labeled (X32 indicates that the residue varies in sequence).

nearby protein molecule (a non-crystallographic symmetry-related DsbA protein), this change in polar side chain conformation could represent a change that occurs upon interaction of DsbA with a protein substrate. The significance of such a conformational change is unclear but, at the least, the conformation observed in monomer B of *wt* DsbA may be required for substrate access to Cys30.

Also, the DsbA mutant structures show that the stability changes resulting from His32 modification are not a result of an altered active-site structure, nor to a change in solvent structure at the active site. Thus, the precise structure of the active-site disulfide of DsbA is retained in the structures of the oxidized His32 mutants. Furthermore, two water molecules, which may be involved in stabilizing the catalytic Cys30 side chain, are highly conserved in the DsbA *wt* and His32 mutant structures. One of these waters interacts through a hydrogen bond with residue 32, yet is found in the DsbA structure whether residue 32 is a histidine, a tyrosine, a leucine, or a serine. The functional role, if any, of these waters is not known though both would probably need to be displaced to allow the formation of a mixed disulfide between DsbA and polypeptide substrate.

Overall, the structural results support the possibility that His32 destabilizes oxidized DsbA at pH 7, not through a conformational effect but through an electrostatic effect. A destabilizing electrostatic effect for the equivalent histidine in oxidized PDI has been proposed (Kortemme et al., 1996). The important contributors at the active site to electrostatic differences between the oxidized and reduced states of DsbA and PDI appear to be the thiolate anion of Cys30, the partial positive charge generated at the N-terminus of the helix dipole (Hol et al., 1978), and the histidine situated between the two active-site cysteines. The Cys30 thiolate anion is present only in the reduced form of these proteins, while the helix dipole is likely to be a factor in both the reduced and oxidized forms. The pK_a of His32 in oxidized DsbA is not known. However, the destabilizing effect of the equivalent histidine in oxidized PDI

is observed as a lowered pK_a (Kortemme et al., 1996) and this could also be true for His32 in DsbA. In reduced DsbA, the active-site histidine may be at least partially charged at physiological pH, through a favorable interaction with the thiolate anion of Cys30. The relative stability of reduced DsbA or PDI compared to their respective oxidized forms can thus be explained, at least in part, in terms of electrostatic stabilization of the Cys30 thiolate through favorable interaction with the partial positive charges of the helix dipole and possibly the active-site histidine in the reduced enzyme (Kortemme et al., 1996) and an unfavorable interaction between the histidine and the helix dipole in the oxidized enzyme.

In the oxidized form, replacement of His32 of DsbA with tyrosine, leucine, or serine results in an increase in stability of ~5–7 kcal/mol (Table 1) compared with *wt*, oxidized DsbA, but there is no concomitant change in structure. The stabilization of the oxidized form is greatest when His32 is replaced with a tyrosine (H32Y) rather than with leucine (H32L) or serine (H32S). The higher stability of the oxidized glutaredoxin variant H32Y DsbA compared with the respective oxidized forms of the other His32 mutants could also be an electrostatic effect since tyrosine can be negatively charged, in principle, while leucine and serine cannot. A negatively charged tyrosine at position 32 could interact favorably with the partial positive charge of the helix dipole—an interaction that is not possible for the other two His32 mutants. Alternatively, the tyrosine at position 32 may be further stabilized compared with the other oxidized His32 mutants through the formation of favorable hydrophobic interactions with Phe36.

The crystal structures of these His32 mutants do not provide conclusive answers to the questions of stability and redox properties of DsbA, particularly in regard to the observed stability changes of the dithiol form. It is possible that a much clearer picture may emerge when the structure of reduced DsbA is known. However, the DsbA mutant structures do show that large conformational changes and changes in active-site solvent structure can be ruled

out as possible mechanisms by which His32 destabilizes the oxidized form of *wt* DsbA. Consequently, the results presented here support the argument that active-site electrostatics play an important role in determining the stability and redox properties of DsbA.

Materials and methods

Measurement of redox equilibrium constants,

Cys30 pK_a and stability

The equilibrium constant between H32Y DsbA and glutathione was measured fluorimetrically using the redox state-dependent fluorescence of DsbA at 330 nm, assuming no significant equilibrium concentrations of DsbA/glutathione-mixed disulfides (Wunderlich & Glockshuber, 1993b). The oxidized protein (1 μ M) was incubated for 16 h at 30 °C in 100 mM sodium phosphate pH 7.0, 1 mM EDTA containing 5–500 μ M GSSG and 1–15000 μ M GSH under nitrogen atmosphere. The true concentration of GSSG in each redox buffer was determined independently with the glutathione reductase assay as described previously (Loferer et al., 1995). The equilibrium constants with glutathione (K_{eq}) were determined by fitting the original fluorescence data according to Equation 1.

$$F = F_{ox} + ([GSH]_2/[GSSG]) \times (F_{red} - F_{ox})/(K_{eq} + [GSH]_2/[GSSG]) \quad (1)$$

where F is the measured fluorescence at 330 nm and F_{ox} and F_{red} are the fluorescence intensities of the oxidized and reduced protein, respectively.

The pH-dependent ionization of the C30 thiol was followed at 30 °C by the specific absorbance of the thiolate at 240 nm (Nelson & Creighton, 1994; Grauschopf et al., 1995; Hennecke et al., 1997). As a control, the pH-dependent absorbance of the oxidized form was recorded. To avoid precipitation artifacts and to minimize buffer absorbance, a buffer consisting of 10 mM K₂HPO₄, 10 mM boric acid, 10 mM sodium succinate, 1 mM EDTA, and 200 mM KCl (containing 100 μ M β -mercaptoethanol for the reduced proteins) was used. The pH (initial value: 8.5) was lowered to 2.2 by stepwise addition of aliquots of 0.1 M HCl and the absorbance at 240 nm and 280 nm was recorded and corrected for the volume increase. Samples had an initial protein concentration of 25 μ M. The pH-dependence of the thiolate-specific absorbance signal ([A240/A280]reduced/[A240/A280]oxidized) was fitted according to the Henderson-Hasselbach equation.

Stability measurements for H32Y DsbA are taken from Wunderlich (1994). Stability measurements for H32S DsbA were performed as described in Grauschopf et al. (1995). Redox equilibrium constants for *wt* DsbA H32S and H32L, and stability measurements and pK_a of Cys30 for *wt* and H32L DsbA are taken from Grauschopf et al. (1995). The Cys30 pK_a value for H32S (P. Korber and J. C. A. Bardwell, unpublished) was measured as previously described for H32L Grauschopf et al. (1995).

Protein production and crystallization

The DsbA variant H32Y was constructed by site-directed mutagenesis according to Kunkel (Kunkel et al., 1987) using single-stranded DNA from the expression plasmid pRBI-PDI (Wunderlich & Glockshuber, 1993a), expressed and purified as described previously (Wunderlich et al., 1995). The H32S and H32L mutants

were identified from an *in vivo* screen for mutants of DsbA with altered redox activity and were prepared as described previously (Grauschopf et al., 1995).

Samples for crystallization of all three His32 DsbA mutants were oxidized using 1.5 mM copper [II] phenanthroline, dialyzed against 20 mM Hepes/NaOH pH 7.5, and purified by FPLC on a HR 5/5 Mono Q column followed by concentration to 20–40 mg/mL. Crystals of the DsbA mutants were grown using the same method used for *wt* DsbA crystals, and are isomorphous with the C2 form *wt* DsbA crystals (Martin et al., 1993b). The unit cell dimensions for H32Y DsbA are $a = 117.7$ Å, $b = 65.1$ Å, $c = 76.4$ Å, $\beta = 126.5^\circ$; for H32L DsbA are $a = 117.7$ Å, $b = 65.1$ Å, $c = 75.9$ Å, $\beta = 126.1^\circ$; and for H32S DsbA are $a = 117.3$ Å, $b = 64.9$ Å, $c = 75.9$ Å, $\beta = 126.1^\circ$.

Crystallographic data collection and processing

Statistics from the crystallographic data processing are presented in Table 2. Data were measured at 16 °C using an RAXIS-IIC imaging plate area detector with RU-200 rotating anode generator. The X-ray generator was operating at 60 kV and 90 mA for H32Y and at 46 kV and 60 mA for H32S and H32L. The crystal to detector distance was 100 mm for H32Y DsbA and 75 mm for H32S and H32L. An oscillation range of 3° was used for H32Y and 2° for H32S and H32L. The exposure time per frame was 30 min for H32Y and H32S, and 20 min for H32L. For H32Y, the frames were integrated, scaled, and merged using the package provided with the RAXIS-IIC system (Higashi, 1990). Data frames for H32S and H32L were processed using DENZO and SCALEPACK (Z. Otwinowski and W. Minor).

Crystallographic refinement of H32 DsbA mutant structures

The coordinates of oxidized *wt* DsbA (refined at a resolution of 1.7 Å (Guddat et al. 1997; PDB accession code 1FVK) were used as the starting model for modeling the His32 mutant structures. Initially, the mutated residue 32 was modeled as alanine. Subsequent difference Fourier analysis clearly established the position of the side chain in all cases, and these side chains were then built into the structure. Model building was performed using O (Jones et al., 1991) and structural refinement was performed using X-PLOR v3.1 (Brünger, 1992b). Positional refinement, individual B-factor refinement, and bulk solvent correction were employed for structure refinement, using standard X-PLOR protocols. Refinement statistics are given in Table 2.

Residues modeled as alanine due to poorly defined side-chain density are: H32Y residues 13, 14, 52, and 148 from both monomers, residues 55 and 164 from monomer A, and residues 7, 47, and 132 from monomer B; H32L residues 13, 14, 52, 55, and 148 from both monomers, residues 7 and 164 from monomer A, and residues 47, 132, and 158 from monomer B; H32S residues 13, 14, 47, 52, 55, and 148 from both monomers, residue 7 from monomer A, and residue 132 from monomer B. Coordinates of H32Y DsbA, H32L DsbA, and H32S DsbA have been deposited with the Brookhaven Protein Data Bank (Bernstein et al., 1977) with accession codes 1FVJ, 1AC1, and 1ACV, respectively. Structure factors have also been deposited but will be held for release for four years.

Acknowledgments

We thank Alun Jones for mass spectrometric analyses. This work was supported by the Deutsche Forschungsgemeinschaft (grants to M.H.-W.,

R.G., and J.C.A.B.), the Bundesministerium für Bildung und Forschung (J.C.A.B.), the ETH Zürich (M.H.-W. and R.G.) and the Australian Research Council (L.W.G. and J.L.M.). J.L.M. is supported by a Queen Elizabeth II Fellowship.

References

- Akiyama Y, Kamitani S, Kusakawa N, Ito K. 1992. In vitro catalysis of oxidative folding of disulfide-bonded proteins by the *Escherichia coli* *dsbA* (*ppfA*) gene product. *J Biol Chem* 267:22440–22445.
- Bardwell JCA, Lee J-O, Jander G, Martin N, Belin D, Beckwith J. 1993. A pathway for disulfide bond formation in vivo. *Proc Natl Acad Sci USA* 90:1038–1042.
- Bardwell JCA, McGovern K, Beckwith J. 1991. Identification of a protein required for disulfide bond formation in vivo. *Cell* 67:581–589.
- Bernstein FC, Koetzle TF, Williams GJB, Edgar F, Meyer J, Brice MD, Rodgers JR, Kennard O, Shimanouchi T, Tasumi M. 1977. The Protein Data Bank: A computer-based archival file for macromolecular structures. *J Mol Biol* 112:535–542.
- Brünger AT. 1992a. Free R value: A novel statistical quantity for assessing the accuracy of crystal structures. *Nature* 355:472–475.
- Brünger AT. 1992b. *X-PLOR (Version 3.1) manual*. New Haven, Connecticut: Yale University.
- Clarke J, Henrick K, Fersht AR. 1995. Disulfide mutants of Barnase I: Changes in stability and structure assessed by biophysical methods and X-ray crystallography. *J Mol Biol* 253:493–504.
- Darby NJ, Creighton TE. 1995. Characterization of the active-site cysteine residues of the thioredoxin-like domains of protein disulfide isomerase. *Biochemistry* 34:16770–16780.
- Edman JC, Ellis L, Blacher RW, Roth RR, Rutter WJ. 1985. Sequence of protein disulphide isomerase and implications of its relationship to thioredoxin. *Nature* 317:267–270.
- Freedman RB. 1989. Protein disulfide isomerase: Multiple roles in the modification of nascent secretory proteins. *Cell* 57:1069–1072.
- Grauskopf U, Winther J, Korber P, Zander T, Dallinger P, Bardwell JCA. 1995. Why is DsbA such an oxidizing disulfide catalyst? *Cell* 83:947–955.
- Guddat LW, Bardwell JCA, Zander T, Martin JL. 1997. The uncharged surface features surrounding the active site of *Escherichia coli* DsbA are conserved and are implicated in peptide binding. *Protein Sci* 6:1148–1156.
- Hennecke J, Spleiss C, Glockshuber R. 1997. Influence of acidic residues and the kink in the active-site helix on the properties of the disulfide oxidoreductase DsbA. *J Biol Chem* 272:189–195.
- Higashi T. 1990. *R-AXIS-II: A program for indexing and processing R-AXIS II imaging plate data*. Danvers, Massachusetts: Rigaku.
- Hol WGJ, van Duijnen PT, Berendsen HJC. 1978. The α -helix dipole and the properties of proteins. *Nature* 273:443–446.
- Jackson SE, Moracci M, El Masry N, Johnson CM, Fersht AR. 1995. Effect of cavity-creating mutations in the hydrophobic core of chymotrypsin inhibitor. *Biochemistry* 32:11259–11269.
- Jones TA, Zou JY, Cowan SW, Kjeldgaard M. 1991. Improved methods for building protein models in electron density maps and the location of errors in these models. *Acta Cryst A47*:110–119.
- Kemmink J, Darby NJ, Dijkstra K, Nilges M, Creighton TE. 1996. Structure determination of the N-terminal thioredoxin-like domain of protein disulfide isomerase using multidimensional heteronuclear $^{13}\text{C}/^{15}\text{N}$ NMR spectroscopy. *Biochemistry* 35:7684–7691.
- Kortemme T, Darby NJ, Creighton TE. 1996. Electrostatic interactions in the active site of the N-terminal thioredoxin-like domain of protein disulfide isomerase. *Biochemistry* 35:14503–14511.
- Krause G, Lundström J, Barea JL, Pueyo de la Cuesta C, Holmgren A. 1991. Mimicking the active site of protein disulfide isomerase by substitution of proline-34 in *Escherichia coli* thioredoxin. *J Biol Chem* 266:9494–9500.
- Kunkel TA, Roberts JD, Zakour RA. 1987. Rapid and efficient site-specific mutagenesis without phenotypic selection. *Meth Enzymol* 154:367–382.
- Lin T-Y, Kim PS. 1989. Urea dependence of thiol-disulfide equilibria in thioredoxin: Confirmation of the linkage relationship and a sensitive assay for structure. *Biochemistry* 28:5282–5287.
- Loferer H, Wunderlich M, Hennecke H, Glockshuber R. 1995. A bacterial thioredoxin-like protein that is exposed to the periplasm has redox properties comparable with those of cytoplasmic thioredoxins. *J Biol Chem* 270:26178–26183.
- Lundström J, Holmgren A. 1993. Determination of the reduction-oxidation potential of the thioredoxin-like domains of protein disulfide isomerase from the equilibrium with glutathione and thioredoxin. *Biochemistry* 32:6649–6655.
- Martin JL, Bardwell JCA, Kuriyan J. 1993a. Crystal structure of the DsbA protein required for disulphide bond formation in vivo. *Nature* 365:464–468.
- Martin JL, Waksman G, Bardwell JCA, Beckwith J, Kuriyan J. 1993b. Crystallization of DsbA, an *Escherichia coli* protein required for disulphide bond formation in vivo. *J Mol Biol* 230:1097–1100.
- Matthews BW. 1995. Studies on protein stability with T4 lysozyme. *Adv Prot Chem* 46:249–278.
- McGregor MJ, Islam SA, Sternberg MJE. 1987. Analysis of the relationship between side-chain conformation and secondary structure in globular proteins. *J Mol Biol* 198:295–310.
- Nelson JW, Creighton TE. 1994. Reactivity and ionization of the active site cysteine residues of DsbA, a protein required for disulfide bond formation in vivo. *Biochemistry* 33:5974–5983.
- Ponder JW, Richards FM. 1987. Tertiary templates for proteins: Use of packing criteria in the enumeration of allowed sequences for different structural classes. *J Mol Biol* 193:775–791.
- Richardson JS, Richardson DC. 1988. Amino acid preferences for specific locations at the ends of α -helices. *Science* 240:1648–1652.
- Srinivasan N, Sowdhamini R, Ramakrishnan C, Balaram P. 1990. Conformations of disulfide bridges in proteins. *Int J Peptide Protein Res* 36:147–155.
- Wunderlich M. 1994. Bakterielle Protein-Disulfid-Isomerase (Dsbft): Redox-eigenschaften und Katalyse oxidativer Proteinfaltung. [Ph.D. thesis] Regensburg, Germany: University of Regensburg.
- Wunderlich M, Glockshuber R. 1993a. In vivo control of redox potential during protein folding catalyzed by bacterial protein disulfide isomerase (DsbA). *J Biol Chem* 268:24547–24550.
- Wunderlich M, Glockshuber R. 1993b. Redox properties of protein disulfide isomerase (DsbA) from *Escherichia coli*. *Protein Sci* 2:717–726.
- Wunderlich M, Jaenicke R, Glockshuber R. 1993. The redox properties of protein disulfide isomerase (DsbA) of *Escherichia coli* result from a tense conformation of its oxidized form. *J Mol Biol* 233:559–566.
- Wunderlich M, Otto A, Maskos K, Mucke M, Seckler R, Glockshuber R. 1995. Efficient catalysis of disulfide formation during protein folding with a single active-site cysteine. *J Mol Biol* 247:28–33.
- Zapun A, Bardwell JCA, Creighton TE. 1993. The reactive and destabilising disulfide bond of DsbA, a protein required for protein disulfide bond formation in vivo. *Biochemistry* 32:5083–5092.